J. Plasma Phys. (2019), *vol.* 85, 905850110
doi:10.1017/S0022377819000011

Dust vortices in a direct current glow discharge plasma: a delicate balance between ion drag and Coulomb force

Sayak Bose[1,2,†], M. Kaur[1,3], P. K. Chattopadhyay[1], J. Ghosh[1], Edward Thomas Jr[4] and Y. C. Saxena[1]

[1]Institute for Plasma Research, HBNI, Bhat, Gandhinangar - 382428, India

[2]Columbia Astrophysics Laboratory, Columbia University, 550 West 120th Street, New York City, NY 10027, USA

[3]Department of Physics and Astronomy, Swarthmore College, Swarthmore, PA 19081, USA

[4]Department of Physics, Auburn University, Auburn, AL 36849, USA

(Received 5 August 2018; revised 4 January 2019; accepted 7 January 2019)

Dust vortices with a void at the centre are reported in this paper. The role of the spatial variation of the plasma potential in the rotation of dust particles is studied in a parallel plate glow discharge plasma. Probe measurements reveal the existence of a local potential minimum in the region of formation of the dust vortex. The minimum in the potential well attracts positively charged ions, while it repels the negatively charged dust particles. Dust rotation is caused by the interplay of the two oppositely directed ion drag and Coulomb forces. The balance between these two forces is found to play a major role in the radial confinement of the dust particles above the cathode surface. Evolution of the dust vortex is studied by increasing the discharge current from 15 to 20 mA. The local minimum of the potential profile is found to coincide with the location of the dust vortex for both values of discharge currents. Additionally, it is found that the size of the dust vortex as well as the void at the centre increases with the discharge current.

Key words: complex plasmas, dusty plasmas

1. Introduction

Dusty plasma consists of electrons, ions, neutrals and macroscopic dust particles that are visible to the naked eye. The dust particles generally acquire large negative charges ($10^3e^- – 10^6e^-$) due to the higher mobility of electrons compared to ions. These highly charged dust particles interact strongly with each other and with the surrounding plasma to give rise to various intriguing collective phenomena at macroscopic scales. Examples include formation of Coulomb crystals (Chu & Lin 1994), formation of voids (Praburam & Goree 1996; Tsytovich *et al.* 2001; Thomas Jr, Avinash & Merlino 2004), formation of dust vortices (Law *et al.* 1998; Laishram, Sharma & Kaw 2014; Kaur *et al.* 2015*a*,*b*), the excitation of waves and instabilities

† Email address for correspondence: sayakbose02@gmail.com

(Rao, Shukla & Yu 1990; Barkan, Merlino & D'angelo 1995; Merlino *et al.* 1998; Samsonov & Goree 1999; Merlino 2014), etc. Study of formation and evolution of vortices is of great interest for enhancing the understanding of basic fluid dynamics (Saffman 1981). In traditional experiments on naturally occurring vortices, it is not possible to observe the interacting particles. However, a dusty plasma provides a unique test-bed to simultaneously study both the vortex dynamics and the trajectory of individual interacting particles constituting the vortices.

In order to study the vortex dynamics, vortices have been produced in dusty plasma in different experimental configurations ranging from direct current (dc) discharge to radio frequency (RF) discharge plasmas (Vaulina *et al.* 2001; Samarian *et al.* 2002), from microgravity conditions to experiments conducted on Earth in the presence of gravity (Akdim & Goedheer 2003; Kaur *et al.* 2016). Different mechanisms, such as non-zero curl of the ion drag force (Kaur *et al.* 2015*a*; Chai & Bellan 2016), presence of a dust charge gradient (Vaulina *et al.* 2004) orthogonal to non-electrostatic forces like ion drag, thermophoretic force, etc., have been put forward to explain the observed dust vortices in different experiments.

We are reporting dust vortices sustained by a balance of two oppositely directed forces, the ion drag force and the Coulomb force ($\boldsymbol{F}_E = Q_d\boldsymbol{E}$, where Q_d is the dust charge, and $\boldsymbol{E}$ is the ambient electric field), in a parallel plate dc glow discharge dusty plasma having a modified cathode geometry. The dust vortices reported in this paper have a dust free region or void at the centre. Probe measurements reveal the existence of a local minimum co-located with the dust vortex. The motion of the dust particles constituting the dust vortex with a void at the centre is studied by correlating the trajectory of the dust particles with variations in background plasma parameters.

The remainder of the paper is organized as follows. In § 2, we briefly describe the experimental set-up used for carrying out these studies. In § 3, we present the experimental results followed by a discussion on the radial confinement and the delicate balance between the ion drag force and the Coulomb force behind the rotation of the dust particles. Finally, a summary is provided in § 4.

2. Experimental set-up

The experiments are carried out in complex plasma experimental device (CPED) (Kaur *et al.* 2016) and its schematic is shown in figure 1. An argon plasma is produced by applying a steady potential difference between two coaxially arranged electrodes separated by 4 cm. The upper electrode serves as an anode, while the lower electrode serves as a cathode, as shown in figure 2(*a*). A metallic ring of inner diameter 6.2 cm and outer diameter 8.2 cm is placed coaxially on the cathode. The height of the ring above the cathode surface is 0.3 cm. More details on the experimental set-up can be found in earlier publications of Kaur *et al.* (2015*a*, 2016).

Plasma is produced in CPED over a wide operating range. The discharge current can be varied from 1 to 50 mA. A maximum potential difference of 1 kV can be applied in between the two electrodes. The experiments are usually carried out at high pressures, $P > 100$ Pa. For the experiments reported in this paper, the discharge current is varied from 15 to 20 mA and the discharge voltage is changed from 400 to 460 V. Pressure is held constant at 167 Pa.

To study the dust vortices, mono-disperse melamine formaldehyde particles of diameter 6.48 ± 0.08 μm are placed on the lower electrode inside the ring. The cathode surface within the metal ring is completely covered by dust particles, as shown in figure 2(*a*). The levitated dust particles are illuminated by a vertical laser

https://doi.org/10.1017/S0022377819000011 Published online by Cambridge University Press

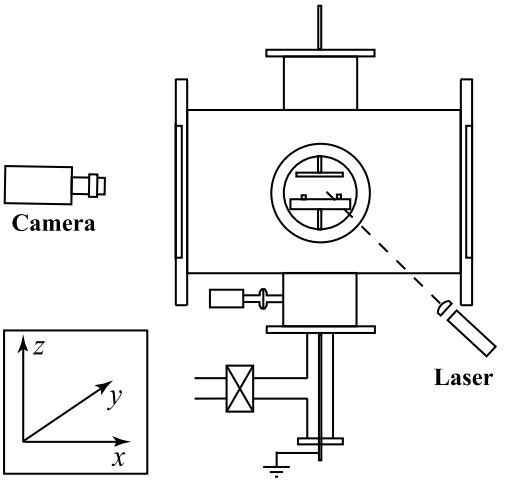

FIGURE 1. Schematic of complex plasma experimental device (side view). The camera has been aligned along the x-axis; the laser sheet is pointed in the y-direction and z represents the vertical direction.

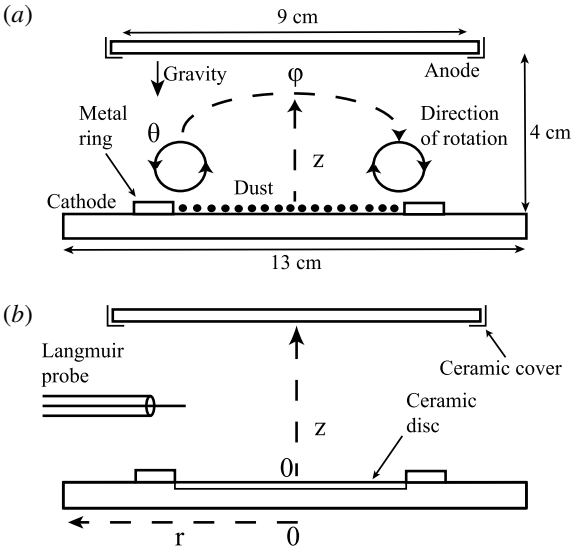

FIGURE 2. (*a*) Schematic of the electrode arrangement and a coordinate representation of dust torus. Here, z represents the direction opposite to gravity, r represents radial direction, ϕ represents the toroidal/azimuthal direction and θ represents the poloidal direction (direction of rotation of dust particles). (*b*) Electrode arrangement and coordinate representation for Langmuir probe measurement.

sheet of thickness 0.2 cm. The laser sheet is obtained using a 532 nm, 100 mW laser followed by a cylindrical lens. The laser light scattered by the dust particles is recorded using an sCMOS camera through one of the axial ports of CPED. The sCMOS camera has a maximum resolution of 2560 pixel × 2160 pixel. For further details on the camera and optical arrangements, refer to Kaur *et al.* (2015*a*, 2016).

https://doi.org/10.1017/S0022377819000011 Published online by Cambridge University Press

An ultra-thin single Langmuir probe of diameter 0.125 mm and length of 6 mm is used for characterization of the plasma (Kaur *et al.* 2015*c*; Bose *et al.* 2017). The electron temperature is determined from the electron retarding exponential region of the I–V characteristics, while the ion density is determined from the ion current. Ion–neutral collisions occur in the probe sheath for probe measurements at 167 Pa neutral pressure and plasma density $\sim 10^9$ cm^{-3}. Collision of ions with neutrals in the sheath surrounding the probe in the OML regime $D_\lambda = r_p/\lambda_D \lesssim 3$ affect the ion collection by the probe in two ways (Schulz & Brown 1955; Bose *et al.* 2017). Orbital destruction of the ions in the sheath results in an increase in the ion current collected by the probe. Elastic scattering of the ions in the probe sheath leads to a decrease in the probe ion current. These two opposing effects are taken into consideration simultaneously by the 'modified TALBOT and CHOU model' (Tichý *et al.* 1994). According to this theory, the ion current collected by the Langmuir probe is expressed as $I_{\text{ion}} = \gamma_1 \gamma_2 I_L$, where, γ_1 accounts for the increase in ion current due to orbital destruction (Zakrzewski & Kopiczynski 1974) and γ_2 accounts for the decrease in ion current due to scattering of ions (Talbot & Chou 1969); I_L is the collisionless Laframboise current (Laframboise 1966). The method of determination of ion density from the ion current using the 'modified TALBOT and CHOU model' is well described by Bose *et al.* (2017).

The Langmuir probe measurements are carried out in the absence of dust particles using a separate cathode. This cathode is identical to that used in experiments in the presence of dust in all respects, except that the dust on the cathode surface is replaced by a ceramic disc, such that the area of the cathode covered by the dielectric (dust particles or ceramic disc) and the exposed metal remains the same. The thickness of the cathode used for plasma production in the absence of dust during Langmuir probe measurements is slightly smaller on the inner side of the metal ring than the cathode used in the presence of dust. This is done to ensure that the cumulative thickness of the cathode does not increase on placing the ceramic disc on the cathode surface during Langmuir probe measurements, as shown in figure 2(*b*). This approach allows high quality probe measurements to be made in a dusty plasma without probe contamination by the dust particles.

The effects of dust on plasma parameters have been measured by other researchers by varying the dust density in laboratory experiments. The results of Adhikary *et al.* (2007) shows that a dust density of $\sim 10^3$ cm^{-3} will not alter the background plasma parameters for a plasma density of $\sim 10^9$ cm^{-3}. In our experiments, the dust density is $\sim 10^3$ cm^{-3} and the plasma density is $\sim 10^9$ cm^{-3}. Therefore, the plasma parameters will not be affected by the presence of dust particles in the experiments reported in this paper.

3. Experimental results and discussion

A poloidally rotating dust structure with toroidal symmetry localized above a metallic ring placed on the cathode surface is observed in an unmagnetized glow discharge plasma (Kaur *et al.* 2015*a*,*b*). The experiments are carried out at high neutral pressure. Initially, at 167 Pa pressure and 15 mA discharge current, a dust torus with a void at the centre is observed. The vertical cross-section illuminated by the laser sheet shows a filled poloidally rotating structure, as shown in figure 3(*a*,*c*). Upon increasing the discharge current to 20 mA, the size of the rotating dust structure increases, as shown in figure 3(*b*,*d*).

Particle image velocimetry (PIV) analysis is performed on the still images using openPIV software to determine the velocity of the dust particles in a two-dimensional

https://doi.org/10.1017/S0022377819000011 Published online by Cambridge University Press

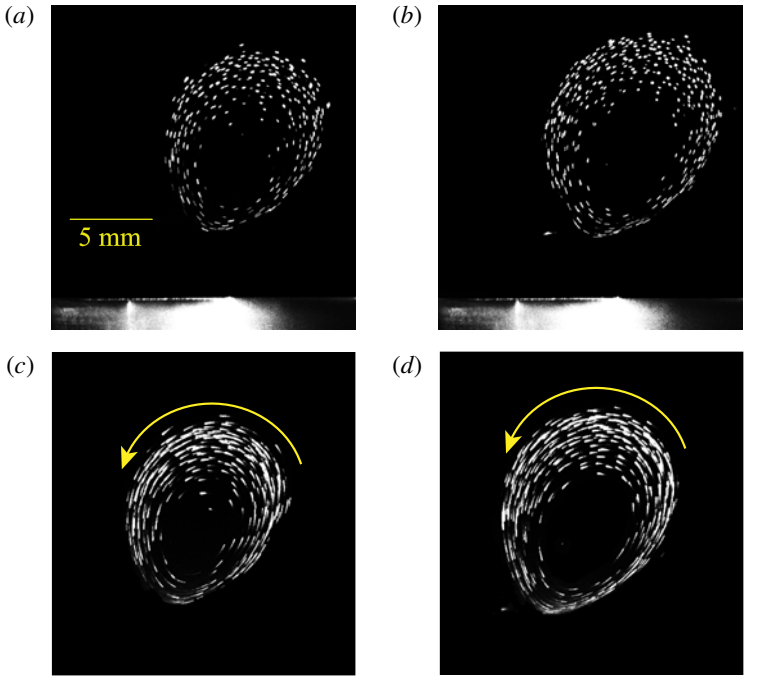

FIGURE 3. Evolution of the dust structure at 167 Pa neutral argon pressure with increase in discharge current. Cross-section of the dust torus at (*a*) 15 mA, and (*b*) 20 mA discharge currents. Superposition of twenty consecutive images of the dust vortex acquired at (*c*) 15 mA, and (*d*) 20 mA discharge current. The yellow arrows in (*c*,*d*) indicate the direction of rotation of the dust particles. The dust vortices shown here correspond to a vortex on the left poloidal pane of the torus in figure 2. The brightness and contrast of the image has been adjusted for better viewing. Please refer to the supplementary material for videos of the rotating dust particles available at https://doi.org/10.1017/S0022377819000011.

r–*z* plane (Taylor *et al.* 2010; Williams 2016). A total of 850 still images of the rotating dust structure are recorded with a sCMOS camera at a resolution 1392 × 1040 pixel at 142.5 frames per second. For PIV analysis, the interrogation window size is taken as 32 × 32 with 16 × 16 overlapping. PIV analysis provides 849 flow fields. These are averaged to determine the mean velocity profile, which represents the velocity profile for the majority of flow fields.

Figure 4, represents the two-dimensional velocity profile of the dust particles at 20 mA discharge current. Peak poloidal velocity (v_θ) of 45 mm s^{-1} is observed from the two-dimensional velocity profile in figure 4 at 20 mA discharge current. However, the velocity measurements from the PIV analysis near the bottom of the rotating dust structure at (150, 50), as shown in figure 4, is an underestimation. This is because the fast moving dust particles move a considerably larger distance in a single exposure time, and hence appear as lines near the bottom of the rotating structure in the still images, as seen in figure 3(*b*). The velocity profiles using PIV analysis are best obtained when the particle moves a small distance, typically less than 30 % across the interrogation box (Thomas Jr 1999). At the bottom location, the dust velocity is determined by taking the ratio of the measured track length of the dust particle in a

https://doi.org/10.1017/S0022377819000011 Published online by Cambridge University Press

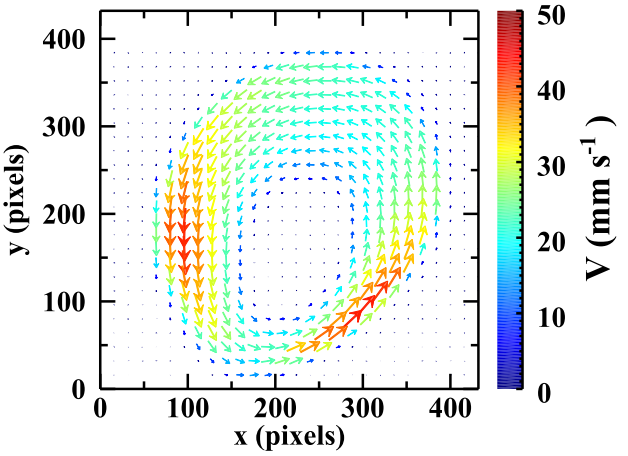

FIGURE 4. The spatial variation of the velocity of the rotating dust particles at 20 mA discharge current. The two-dimensional velocity profiles are an ensemble average of 849 flow fields (850 frames) in the PIV analysis with an interrogation window size of 32×32 with 16×16 overlap. Velocity vectors show the direction of rotation of dust particles; the colour bar represents the value of dust velocity in mm s^{-1}.

single exposure time and the exposure time. Using this method, the dust velocity is found to be $\sim$74 mm s^{-1}.

We have measured plasma parameters at different horizontal and vertical locations using a Langmuir probe for the two discharge currents of 15 mA and 20 mA. Radial density and floating potential profiles measured at different heights for a background neutral pressure of 167 Pa and discharge current 15 mA are shown in figures 5(*a*) and 5(*b*), respectively. Similarly, the density and potential profiles measured at a discharge current of 20 mA are shown in figures 6(*a*) and 6(*b*), respectively. A sharp radial density gradient is observed at the location of the dust vortex, in agreement with our previous observations for dust filled vortices (Kaur *et al.* 2015*a*,*b*). This implies that the momentum transferred to the dust particles by the ion flux from the anode to cathode varies radially. A greater momentum will be transferred by the ions to the dust particles where the density is high near the metal ring kept on the cathode surface, while the ions near the centre of the cathode in the low density region will exert a smaller force on the dust particles.

The electron temperature is approximately constant in the region of formation of dust vortex. The radial variation of electron temperature for two representative heights at 15 mA and 20 mA is shown in figures 7(*a*) and 7(*b*), respectively. Since, the variation of electron temperature is negligible, the spatial variation of the floating potential is considered to follow the spatial variation of the plasma potential.

A local minimum in the radial profile of the floating potential, and hence, in the plasma potential, is observed at lower heights from the cathode surface as shown in figures 6(*a*) and 5(*a*). The local minimum is found to be located near the inner edge of the metal ring kept on the cathode surface coinciding with the location of the dust vortex. The observed local minimum in the radial profile of the floating/plasma potential implies that there is a radial electric field directed towards the minimum. The local minimum will attract the positively charged ions, while it will repel the negatively charged dust particles. The ions moving towards the local minimum will

https://doi.org/10.1017/S0022377819000011 Published online by Cambridge University Press

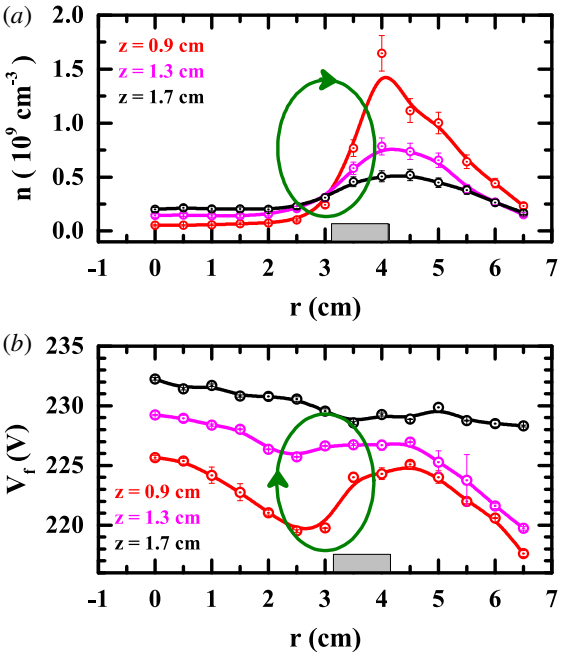

FIGURE 5. (*a*) Radial variation of density and, (*b*) potential profiles measured at a height of 0.9 cm, 1.3 cm and 1.7 cm above the cathode surface. The *r*–*z* plane intersecting the dust torus on the left side from the center of the cathode (marked as 0 in figure 2(*b*)) is sampled by the Langmuir probe. The measurements are carried out at 167 Pa pressure and 15 mA discharge current.

tend to drag negatively charged dust particles along with them, while the Coulomb force will repel the dust particles from the minimum. The presence of a strong monotonic radial density gradient at the location of the local potential minimum implies that the ion drag force is asymmetric about the potential minimum. Thus, it is clear that the forces of electrical origin acting on the charged dust particles have a spatial variation depending on the local values of ion density, electric field, etc.

The effect of forces of electrical origin on the dust vortex is explored by analysing the rotating dust structure with a dust free region at the centre observed at 20 mA discharge current, and 167 Pa neutral pressure, as shown in figure 3(*b*,*d*).

The electrical force experienced by the charged dust particle is a function of the charge of the dust particle and the potential gradient in dc glow discharge in addition to other plasma parameters. The charge is calculated by assuming the dust particle to be a spherical condenser and using the fundamental relation, $Q_d = C_d \Phi_d$, where, Q_d, C_d and Φ_d are the charge, capacitance and surface potential of the dust particle. The surface potential of the dust particle is determined from the balance of the ion and electron flux incident on the dust particle. The experiments are carried out at 167 Pa neutral pressure. At this high pressure, the ion neutral mean free path is 12 μm, which is less than the plasma shielding length for 10^9 cm^{-3} ion density and 1.3 eV electron temperature. However, the electron mean free path, which is two orders larger than the ion mean free path, is also larger than the plasma shielding length. Collisional ion flux incident on the dust particles is calculated using the interpolation formula given by Khrapak & Morfill (2008), while the OML theory, is used to estimate collisionless

https://doi.org/10.1017/S0022377819000011 Published online by Cambridge University Press

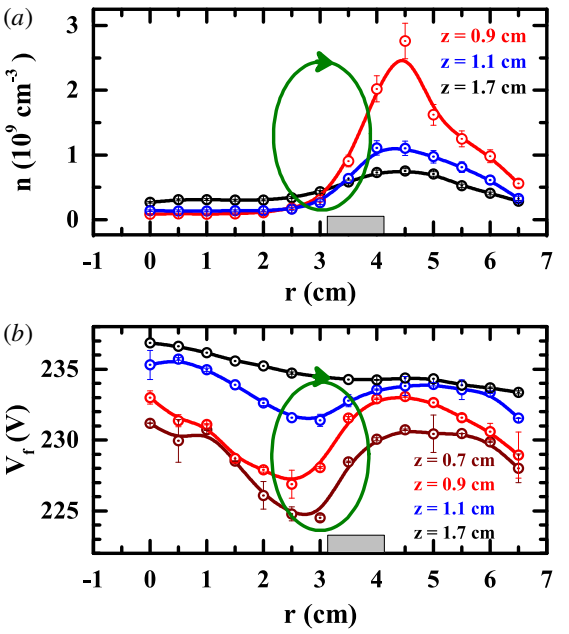

FIGURE 6. (*a*) Radial variation of density and, (*b*) potential profiles measured at a height of 0.7 cm, 0.9 cm, 1.1 cm and 1.7 cm above the cathode surface. The *r*–*z* plane intersecting the dust torus on the left side from the center of the cathode (marked as 0 in figure 2(*b*)) is sampled by the Langmuir probe. The measurements are carried at 167 Pa pressure and 20 mA discharge current.

electron flux. Using the above mentioned formulation, the dust charge is determined to be $4616e^-$ for 10^9 cm^{-3} ion density, 1.3 eV electron temperature, 167 Pa neutral pressure and 6.48 μm dust diameter.

The Coulomb force ($\boldsymbol{F}_E = Q_d\boldsymbol{E}$) acting on the dust particles, as shown in figure 8(*b*,*d*), is determined by multiplying the charge acquired by the dust particles with the local electric field. The value of the electric field is determined from the spatial variation of the floating potential, V_f. The vertical electric field at $z = z_0$ and $r = r_0$ is determined using the formula, $E_z(r_0, z_0) = -\{V(r_0, z_2) - V(r_0, z_1)\}/(z_2 - z_1)$, where $z_2 = z_0 + 0.2$ cm and $z_1 = z_0 - 0.2$ cm. And the radial electric field at $z = z_0$ and $r = r_0$ is determined using a similar formula $E_r(r_0, z_0) = -\{V(r_2, z_0) - V(r_1, z_0)\}/(r_2 - r_1)$, where $r_2 = r_0 + 0.25$ cm and $r_1 = r_0 - 0.25$ cm. For example, using the above mentioned method the radial electric field at $r = 3.5$ cm and $z = 0.9$ cm is determined to be $\boldsymbol{E}_r(r = 3.5 \text{ cm}, z = 0.9 \text{ cm}) = -(232.1 - 229.8)/0.5 = -4.6$ V cm$^{-1}\hat{r}$. Therefore, for a dust charge of $4616e^-$ and electric field $= -4.6$ V cm^{-1}, the Coulomb force turns out to be $\sim 3.4 \times 10^{-13}$ N.

The ion flow results in transfer of momentum from ions to negatively charged dust particles. The drift velocity of the ions due to the presence of an electric field is $\boldsymbol{v}_{\text{Di}} = \mu\boldsymbol{E}$. Mobility is determined using the formula $\mu = \mu_0\{1 + a(E/P)\}^{-1/2}$, where E is the electric field in V cm^{-1}, P is the pressure in torr and 'μ_0' and 'a' are constants (Frost 1957). For argon discharge, 'μ_0' is equal to 1460 cm^2 V^{-1} s^{-1} and 'a' is equal to 0.0264 torr cm V^{-1}. At 167 Pa neutral pressure, the ion neutral collisions occur rather frequently, the ion drag force for subthermal ion flow with $l_i \leqslant \beta_T\lambda$ is given by

https://doi.org/10.1017/S0022377819000011 Published online by Cambridge University Press

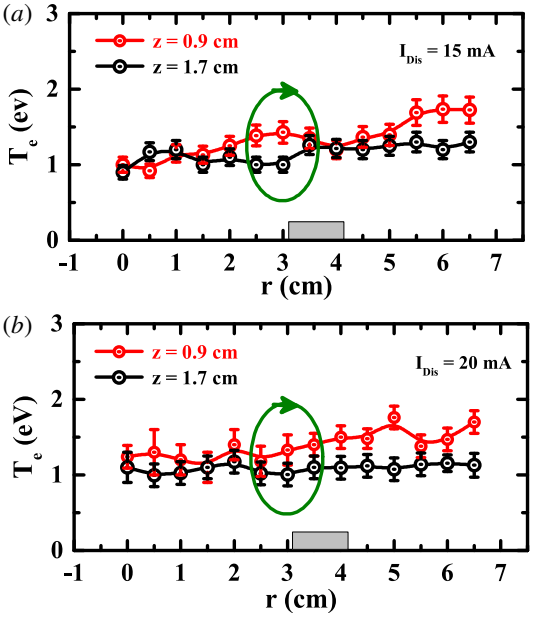

FIGURE 7. Radial variation of electron temperature measured at a height of 0.9 cm and 1.7 cm above the cathode at (*a*) 15 mA and (*b*) 20 mA discharge currents. The measurements are carried out using a Langmuir probe. The *r*–*z* plane intersecting the dust torus on the left side from the center of the cathode (marked as 0 in figure 2(*b*)) is sampled by the Langmuir probe.

Ivlev *et al.* (2004, 2005), Fortov & Morfill (2010) and Kaur *et al.* (2015*a*) as

$$F_{\mathrm{id}} \simeq \frac{1}{6}\left(\frac{T_i}{e}\right)^2\left(\frac{\lambda}{l_i}\right)\beta_T^2 M_T, \tag{3.1}$$

where l_i is the ion mean free path, $M_T(=v_{\mathrm{Di}}/v_{\mathrm{Ti}})$ is the thermal Mach number, $\beta_T(=e^2Z/\lambda T_i)$ is the thermal scattering parameter and λ is the effective screening length. The ion drag force, F_{id}, calculated using (3.1) for ion density 10^9 cm^{-3}, electron temperature $T_e = 1.3$ eV, ion temperature $T_i = 0.03$ eV, electric field $E = 4.6$ V cm^{-1} and at neutral pressure 167 Pa is $\sim 5 \times 10^{-13}$ N. The value of the electric field used in the calculation of the ion drag force is determined from the radial variation of the floating potential.

The neutral frictional force experienced by the dust particle as it wades through the stationary neutral background is estimated using the formula (Epstein 1924; Liu *et al.* 2003)

$$F_{\mathrm{nd}} = \delta\frac{4\pi}{3}n_n m_d r_d^2 \bar{c} v_d, \tag{3.2}$$

where m_d, n_n, r_d, $\bar{c}$ and v_d are the dust mass, neutral density, radius of the dust particle, mean thermal speed of gas atom and dust velocity, respectively. In our experiment $r_d = 3.24$ μm and $m_d = 2.15 \times 10^{-13}$ kg. At 167 Pa neutral pressure and neutral temperature, $T_n \approx 0.03$ eV, the neutral density is estimated to be 3.48×10^{16} cm^{-3}.

https://doi.org/10.1017/S0022377819000011 Published online by Cambridge University Press

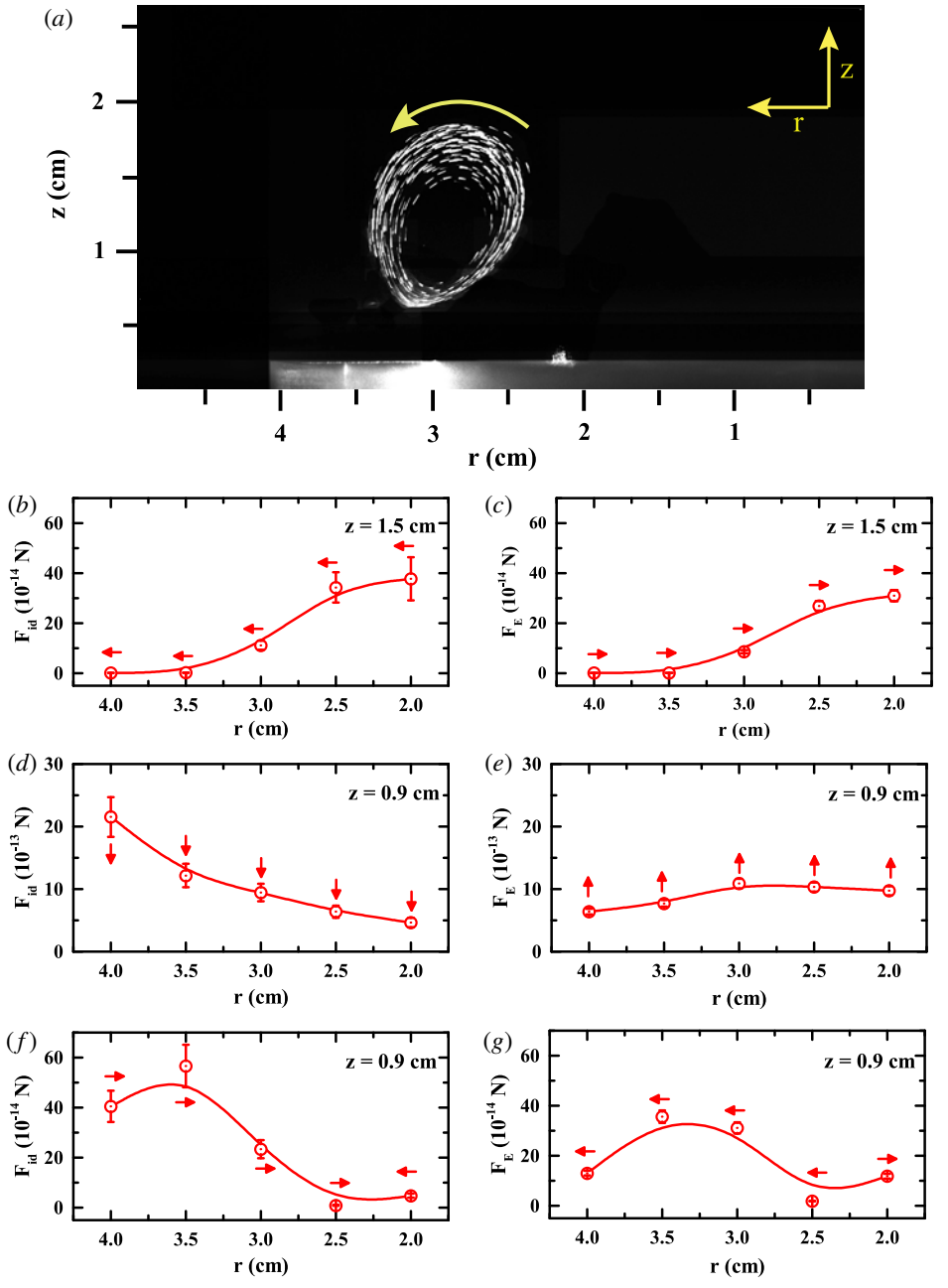

FIGURE 8. (*a*) Superposition of multiple consecutive images of the dust vortex acquired at 20 mA discharge current and 167 Pa neutral pressure. The brightness and contrast of the image has been adjusted for better viewing. The direction of dust rotation is indicated by the curved yellow arrow and the coordinate system is defined in the upper right corner of the image. (*b*,*c*) Show a radial profile of the radial components of the ion drag and Coulomb force, respectively, at a height of 1.5 cm above the cathode surface. A radial profile of the vertical component of the ion drag force and the Coulomb force at a height of 0.9 cm are shown in (*d*,*e*), respectively, and the same for their radial components are plotted in (*f*,*g*), respectively.

https://doi.org/10.1017/S0022377819000011 Published online by Cambridge University Press

Therefore, the corresponding neutral frictional force acting on a dust particle traversing with a speed 5 mm s^{-1} for $\delta = 1$ is $\sim 2 \times 10^{-13}$ N.

Among all the forces, gravity is one of the major forces. The downward directed gravitational force acting on the spherical melamine formaldehyde particle of mass 2.15×10^{-13} kg is 2.1×10^{-12} N.

The Coulomb and ion drag forces acting near the top of the vortex at a height of 1.5 cm, spanning the radial extent covered by the rotating dust particles, are shown in figure 8(*b*,*c*). The direction and the magnitude of these forces near the base of the vortex at a height of 0.9 cm are shown in figure 8(*d*–*f*). These Coulomb and ion drag forces are determined as described previously in this paper by making use of local parameters like density, electric field, etc. These calculations are done to understand the relative importance of the forces of electrical origin on the trajectory of dust particles.

The radial variation of the ion drag and Coulomb force acting on dust particles at a height of $z = 1.5$ cm are shown in figures 8(*b*) and 8(*c*), respectively. The radially outward ion drag force ($F_{\mathrm{id}_r}\hat{r}$) is greater than the radially inward Coulomb force ($F_{\mathrm{E}_r}\hat{r}$). The direction of the effective electrical force, i.e. $F_{\mathrm{id}_r}\hat{r} - F_{\mathrm{E}_r}\hat{r}$ is consistent with the direction of motion of the dust particles.

The downward directed ion drag forces and the upward directed Coulomb forces at $z = 0.9$ cm are shown in figure 8(*d*,*e*). The downward directed ion drag force clearly dominates the Coulomb force near the metal ring, but away from the inner edge of the ring at $r = 2$ cm the upward directed Coulomb force dominates over the downward directed ion drag force. However, the upward directed Coulomb force at $r = 2$ cm is insufficient to balance the force of gravity acting on the dust particles. The radial component of the ion drag and Coulomb force at $z = 0.9$ cm height are shown figure 8(*f*,*g*). The radially inward ion drag force ($-F_{\mathrm{id}_r}\hat{r}$) dominates over the outward directed Coulomb force ($F_{\mathrm{E}_r}\hat{r}$) at $r = 4$ cm, while the radially outward Coulomb force becomes comparable to the oppositely directed ion drag force at $r = 2.5$ cm.

Therefore, we can describe the motion of the dust particles in the vortex using the following descriptions. The dust particles approach the cathode sheath edge under the combined action of the downward directed ion drag and gravity near the metal ring. The downward directed dust particles near the edge of the metal ring experience a radially inward ion drag force (refer figure 8*f*,*g*), which imparts momentum in the radially inward direction to the dust particles. Thus, the dust particles approaching the sheath gains momentum both in the radial ($-\hat{r}$) and in the vertically downward direction ($-\hat{z}$) at the inner edge of the metal ring. The downward approaching dust particles enter the sheath under the action of a dominating ion drag force ($-F_{\mathrm{id}_z}\hat{z} - F_{\mathrm{id}_r}\hat{r}$), these dust particles are ultimately reflected back by the Coulomb force exerted by the strong sheath electric field and gain a momentum in the upward direction. By the time the dust particles gain a momentum in the upward direction, they have already moved radially inwards due to their radial momentum. The dust particles rise above the sheath surface at a radially inward location (away from the inner edge of the metallic ring) making an angle with the vertical. The radial momentum of the dust particles emerging from the sheath in the $-\hat{r}$ direction is opposed by the neutral frictional force leading to a reduction in the radial momentum in the $-\hat{r}$ direction. The vertically upward directed momentum of the dust particles decreases as they rise above the sheath edge. The downward directed gravity, neutral friction and ion drag force impede the vertically upward momentum of the dust particles and finally cause the dust particles to fall towards the cathode surface.

Thus, it can be concluded that the confinement of the dust particles in the region above the metal ring is due to the cumulative action of the ion drag force,

https://doi.org/10.1017/S0022377819000011 Published online by Cambridge University Press

Coulomb force, neutral friction and gravitational force. The rotation of the dust particles is driven by the combined action of the ion drag force and Coulomb force acting on the dust particles.

A comparison of radial ion density profiles (refer to figures 5*a* and 6*a*) for two values of discharge current shows that the ion density increases when the discharge current is increased from 15 to 20 mA. The ion densities in the region where the rotating dust particles approach the cathode surface at $z = 0.9$ cm and $r = 3.5$ cm are 7.6×10^8 cm^{-3} and 9×10^8 cm^{-3} at 15 mA and 20 mA discharge current, respectively. This implies that the ion flux towards the cathode will impart a greater momentum to the dust particles at higher discharge current. This will cause the dust particles to penetrate further into the sheath region resulting in a stronger upward momentum from the cathode sheath field, causing an increase in the size of the vortex. A closer look at figure 3(*a*,*b*) does show that the distance between the bottom edge of the vortex and the metal ring on the cathode indeed decreases with increase in discharge current. At 15 mA and 20 mA discharge currents, the bottoms of the rotating vortex are 4 mm and 3.6 mm, respectively, from the metallic ring on the cathode.

4. Summary

The crucial role played by the spatial inhomogeneity of floating/plasma potential in confining and aiding the rotation of dust particles in a dc glow discharge plasma is presented in this paper. Dust vortex with a void in the centre is produced in a parallel plate dc glow discharge dusty plasma with a modified cathode geometry. A local minimum in the radial profile of the floating potential is observed at lower heights from the cathode surface at the location of formation of the dust vortex. The floating potential is considered to follow the plasma potential because the electron temperature is found to be constant. The local minimum of the floating potential attracts the positively charged ions but repels the negatively charged dust particles. The radial ion density profile exhibits a strong gradient in the region of formation of the dust vortex, resulting in an asymmetric radial variation of the ion density about the local potential minimum. As a result, the ion drag force dominates the Coulomb force at one side of the potential minimum, while the Coulomb force dominates over the ion drag on the other side of the potential minimum. A delicate balance between these two oppositely directed forces is found to play a crucial role in controlling the trajectory of the rotating dust particles.

Another crucial aspect of the dust vortex that this paper addresses is the reason for confinement of the rotating dust particles in the region above the metal ring on the cathode surface. We have shown by logical arguments and by determining the magnitude and direction of the relevant forces that the rotating dust particles are confined by the cumulative action of ion drag force, Coulomb force, neutral friction and force of gravity.

The evolution of the dust vortex is studied by increasing the discharge current from 15 to 20 mA. The local minimum of the potential profile is found to coincide with the location of dust vortex for both values of the discharge current. However, the size of the dust vortex and the void at the centre of the vortex is found to increase with discharge current.

Supplementary movies

Supplementary movies are available at https://doi.org/10.1017/S0022377819000011.

REFERENCES

ADHIKARY, N. C., BAILUNG, H., PAL, A. R., CHUTIA, J. & NAKAMURA, Y. 2007 Observation of sheath modification in laboratory dusty plasma. *Phys. Plasmas* **14** (10), 103705.

AKDIM, M. R. & GOEDHEER, W. J. 2003 Modeling of self-excited dust vortices in complex plasmas under microgravity. *Phys. Rev.* E **67** (5), 056405.

BARKAN, A., MERLINO, R. L. & D'ANGELO, N. 1995 Laboratory observation of the dust-acoustic wave mode. *Phys. Plasmas* **2** (10), 3563–3565.

BOSE, S., KAUR, M., CHATTOPADHYAY, P. K., GHOSH, J., SAXENA, Y. C. & PAL, R. 2017 Langmuir probe in collisionless and collisional plasma including dusty plasma. *J. Plasma Phys.* **83** (2), 615830201.

CHAI, K.-B. & BELLAN, P. M. 2016 Vortex motion of dust particles due to non-conservative ion drag force in a plasma. *Phys. Plasmas* **23** (2), 023701.

CHU, J. H. & LIN, I. 1994 Direct observation of Coulomb crystals and liquids in strongly coupled RF dusty plasmas. *Phys. Rev. Lett.* **72** (25), 4009.

EPSTEIN, P. S. 1924 On the resistance experienced by spheres in their motion through gases. *Phys. Rev.* **23** (6), 710.

FORTOV, V. E. & MORFILL, G. E. 2010 *Complex and Dusty Plasmas: From Laboratory to Space*. CRC Press.

FROST, L. S. 1957 Effect of variable ionic mobility on ambipolar diffusion. *Phys. Rev.* **105**, 354–356.

IVLEV, A. V., KHRAPAK, S. A., ZHDANOV, S. K., MORFILL, G. E. & JOYCE, G. 2004 Force on a charged test particle in a collisional flowing plasma. *Phys. Rev. Lett.* **92**, 205007.

IVLEV, A. V., ZHDANOV, S. K., KHRAPAK, S. A. & MORFILL, G. E. 2005 Kinetic approach for the ion drag force in a collisional plasma. *Phys. Rev.* E **71**, 016405.

KAUR, M., BOSE, S., CHATTOPADHYAY, P. K., GHOSH, J. & SAXENA, Y. C. 2016 Complex plasma experimental device – a test bed for studying dust vortices and other collective phenomena. *Pramana* **87** (6), 89.

KAUR, M., BOSE, S., CHATTOPADHYAY, P. K., SHARMA, D., GHOSH, J. & SAXENA, Y. C. 2015*a* Observation of dust torus with poloidal rotation in direct current glow discharge plasma. *Phys. Plasmas* **22** (3), 033703.

KAUR, M., BOSE, S., CHATTOPADHYAY, P. K., SHARMA, D., GHOSH, J., SAXENA, Y. C. & THOMAS, E. JR. 2015*b* Generation of multiple toroidal dust vortices by a non-monotonic density gradient in a direct current glow discharge plasma. *Phys. Plasmas* **22** (9), 093702.

KAUR, M., BOSE, S., CHATTOPADHYAY, P. K., GHOSH, J. & SAXENA, Y. C. 2015*c* Resolving issues associated with Langmuir probe measurements in high pressure complex (dusty) plasmas. In *Proceedings of the Tenth Asia Plasma and Fusion Association Conference*, p. 168.

KHRAPAK, S. A. & MORFILL, G. E. 2008 An interpolation formula for the ion flux to a small particle in collisional plasmas. *Phys. Plasmas* **15** (11), 114503.

LAFRAMBOISE, J. G. 1966 Theory of spherical and cylindrical Langmuir probes in a collisionless, maxwellian plasma at rest. *Tech. Rep.* DTIC Document.

LAISHRAM, M., SHARMA, D. & KAW, P. K. 2014 Dynamics of a confined dusty fluid in a sheared ion flow. *Phys. Plasmas* **21** (7), 073703.

LAW, D. A., STEEL, W. H., ANNARATONE, B. M. & ALLEN, J. E. 1998 Probe-induced particle circulation in a plasma crystal. *Phys. Rev. Lett.* **80**, 4189–4192.

LIU, B., GOREE, J., NOSENKO, V. & BOUFENDI, L. 2003 Radiation pressure and gas drag forces on a melamine-formaldehyde microsphere in a dusty plasma. *Phys. Plasmas* **10** (1), 9–20.

MERLINO, R. L., BARKAN, A., THOMPSON, C. & D'ANGELO, N. 1998 Laboratory studies of waves and instabilities in dusty plasmas. *Phys. Plasmas* **5** (5), 1607–1614.

MERLINO, R. L. 2014 25 years of dust acoustic waves. *J. Plasma Phys.* **80** (6), 773–786.

PRABURAM, G. & GOREE, J. 1996 Experimental observation of very low-frequency macroscopic modes in a dusty plasma. *Phys. Plasmas* **3** (4), 1212–1219.

RAO, N. N., SHUKLA, P. K. & YU, M. Y. 1990 Dust-acoustic waves in dusty plasmas. *Planet. Space Sci.* **38** (4), 543–546.

SAFFMAN, P. G. 1981 Dynamics of vorticity. *J. Fluid Mech.* **106**, 49–58.

SAMARIAN, A., VAULINA, O., TSANG, W. & JAMES, B. W. 2002 Formation of vertical and horizontal dust vortexes in an RF-discharge plasma. *Phys. Scr.* **2002** (T98), 123.

SAMSONOV, D. & GOREE, J. 1999 Instabilities in a dusty plasma with ion drag and ionization. *Phys. Rev.* E **59** (1), 1047.

SCHULZ, G. J. & BROWN, S. C. 1955 Microwave study of positive ion collection by probes. *Phys. Rev.* **98**, 1642–1649.

TALBOT, L. & CHOU, Y. S. 1969 Langmuir probe response in the transition regime. In *Rarefied Gas Dynamics*, vol. II, pp. 1723–1737. Academic.

TAYLOR, Z. J., GURKA, R., KOPP, G. A. & LIBERZON, A. 2010 Long-duration time-resolved PIV to study unsteady aerodynamics. *IEEE Trans. Instrument. Meas.* **59** (12), 3262–3269.

THOMAS, E. JR. 1999 Direct measurements of two-dimensional velocity profiles in direct current glow discharge dusty plasmas. *Phys. Plasmas* **6** (7), 2672–2675.

THOMAS, E. JR., AVINASH, K. & MERLINO, R. L. 2004 Probe induced voids in a dusty plasma. *Phys. Plasmas* **11** (5), 1770–1774.

TICHÝ, M., ŠÍCHA, M., DAVID, P. & DAVID, T. 1994 A collisional model of the positive ion collection by a cylindrical Langmuir probe. *Contrib. Plasma Phys.* **34** (1), 59–68.

TSYTOVICH, V. N., VLADIMIROV, S. V., MORFILL, G. E. & GOREE, J. 2001 Theory of collision-dominated dust voids in plasmas. *Phys. Rev.* E **63**, 056609.

VAULINA, O. S., PETROV, O. F., FORTOV, V. E., MORFILL, G. E., THOMAS, H. M., SEMENOV, Y. P., IVANOV, A. I., KRIKALEV, S. K. & GIDZENKO, Y. P. 2004 Analysis of dust vortex dynamics in gas discharge plasma. *Phys. Scr.* **2004** (T107), 224.

VAULINA, O. S., SAMARIAN, A. A., NEFEDOV, A. P. & FORTOV, V. E. 2001 Self-excited motion of dust particles in a inhomogeneous plasma. *Phys. Lett.* A **289** (4), 240–244.

WILLIAMS, J. D. 2016 Application of particle image velocimetry to dusty plasma systems. *J. Plasma Phys.* **82** (3), 615820302.

ZAKRZEWSKI, Z. & KOPICZYNSKI, T. 1974 Effect of collisions on positive ion collection by a cylindrical Langmuir probe. *Plasma Physics* **16** (12), 1195.